

Supplementary Information:

High-Performance Solution-Processed Red Hyperfluorescent OLEDs Based on Cibalackrot

Nicholle R. Wallwork,^{a,b} Masashi Mamada,^{c,*} Atul Shukla,^{a,d} Sarah K. M. McGregor,^{a,b}
Chihaya Adachi,^{c,d,*} Ebinazar B. Namdas^{a,e,*} and Shih-Chun Lo^{a,b,*}

^a *Centre for Organic Photonics & Electronics, The University of Queensland, Brisbane, Queensland, 4072, Australia*

^b *School of Chemistry and Molecular Biosciences, The University of Queensland, Brisbane, Queensland, 4072, Queensland, Australia*

^c *Centre for Organic Photonics and Electronics Research (OPERA), Kyushu University, 744 Motoooka, Nishi, Fukuoka 819-0395, Japan*

^d *International Institute for Carbon Neutral Energy Research (WPI-I2CNER), Kyushu University, 744 Motoooka, Nishi, Fukuoka 819-0395, Japan*

^e *School of Mathematics and Physics, The University of Queensland, Queensland, Brisbane, Queensland, 4072, Australia*

Table of Contents

Table S1 Photophysical properties in solution.....	2
Table S2 Photophysical properties in neat films.....	2
Table S3 Photophysical properties of Cibalackrot B blend films	6
Figure S1 UV-Vis absorption, fluorescence, and phosphorescence of compounds in solution and neat film.....	3
Figure S2 Normalised absorption, and PL spectra of thin films containing varying mol% of Cibalackrot with TADF material 4CzIPN or 4CzIPN- ^t Bu.....	4
Figure S3 Solid state TCSPC prompt and delayed fluorescence decay of thin films	5
Figure S4 EQEs (%) (>100 cd m ⁻²) of hyperfluorescent OLEDs <i>versus</i> electroluminescent peak wavelength (λ_{EL}) (nm).	6
References.	7

Table S1 Photophysical properties in solution

Compound ^a	λ_{abs} (nm) ^b	$E_{\text{g}}^{\text{opt}}$ (eV) ^c	λ_{fluo} (nm) ^b	S_1 (eV) ^c	λ_{phos} (nm) ^d	T_1 (eV) ^c	ΔE_{ST} (eV)
CBP	294, 327, 340	3.52	366	3.56	487, 512	2.77	0.79
4CzIPN- ^t Bu	280, 387, 467	2.53	525	2.61 (2.61) ^e	502	2.61	<0.01
4CzIPN	281, 374, 449	2.65	512	2.70 (2.69) ^e	496	2.65	0.05
Cibalackrot	281, 527, 567	2.09	594	2.18	– ^f	– ^f	– ^f

^a In toluene. ^b Measured in ambient conditions. ^c Calculated from λ_{onset} . ^d Measured at 77 K with a delay. ^e Values in parenthesis indicate S_1 at 77 K. ^f Could not be detected.

Table S2 Photophysical properties in neat films

Compound ^a	λ_{abs} (nm) ^b	$E_{\text{g}}^{\text{opt}}$ (eV) ^c	λ_{fluo} (nm) ^b	S_1 (eV) ^c	λ_{phos} (nm) ^d	T_1 (eV) ^c	ΔE_{ST} (eV)
CBP	296, 330, 343	3.43	379, 403	3.46	489, 528	2.60	0.86
4CzIPN- ^t Bu	292, 387, 457	2.41	550	2.52 (2.48) ^e	539	2.46	0.06
4CzIPN	289, 381, 452	2.46	568	2.47 (2.43) ^e	553	2.41	0.06

^a Spin-coated onto a quartz substrate from chloroform. ^b Measured in ambient conditions. ^c Calculated from λ_{onset} . ^d Measured at 77 K with a delay. ^e Values in parenthesis indicate S_1 at 77 K.

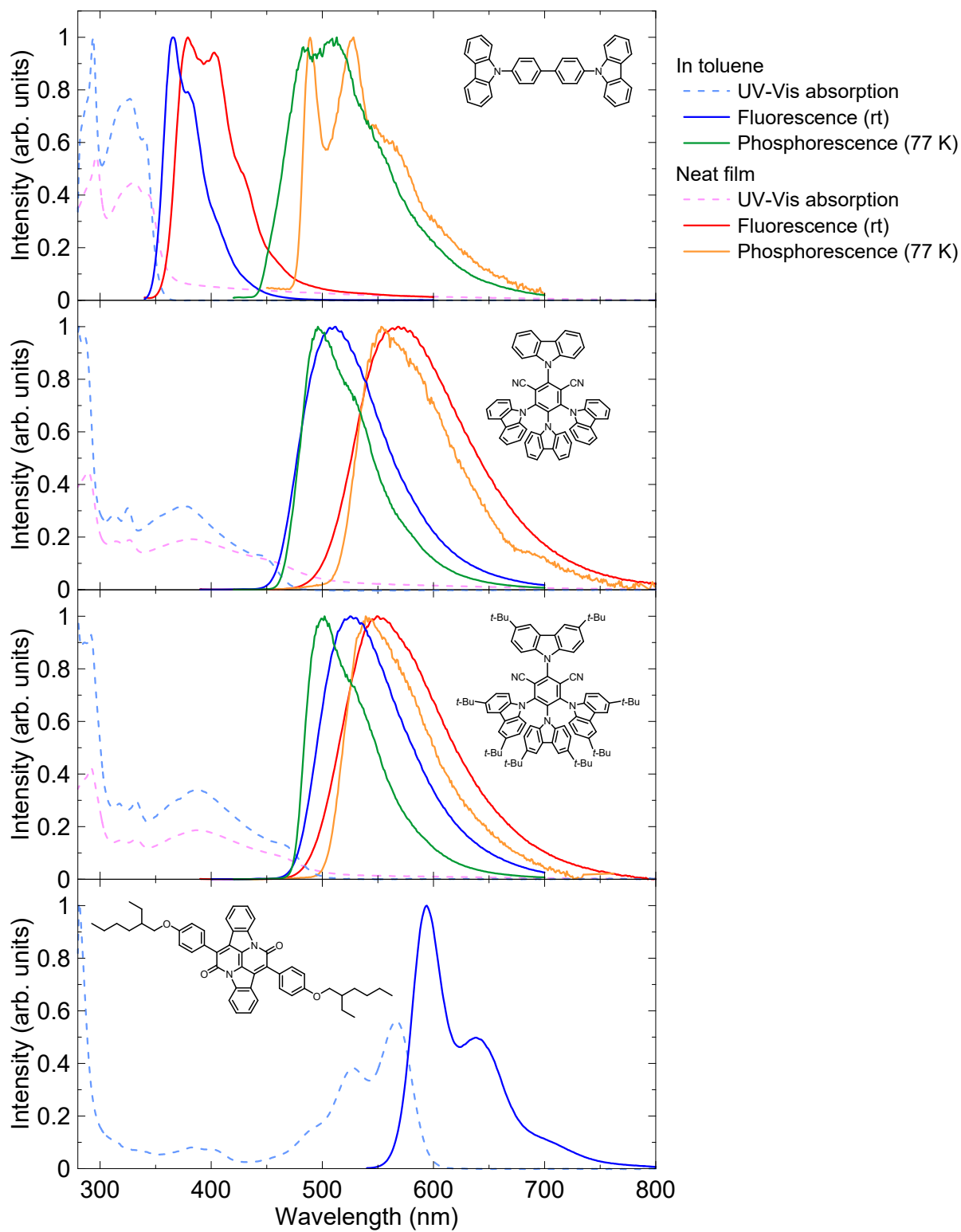


Figure S1 UV-Vis absorption, fluorescence, and phosphorescence of compounds (inset) in solution and neat films.

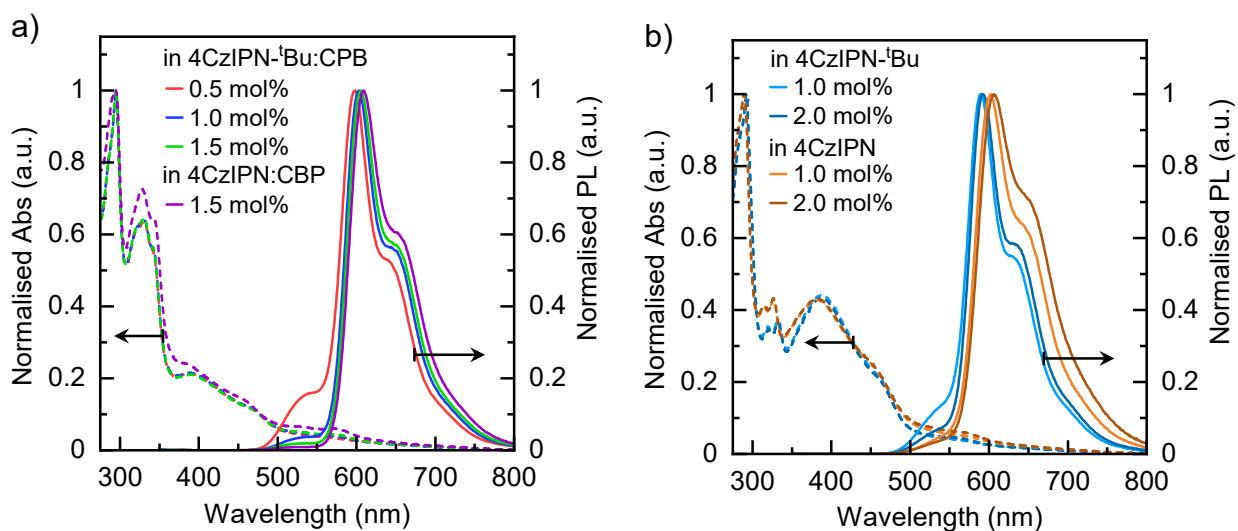


Figure S2 Normalised absorption (dashed lines), and PL (solid lines) spectra of thin films containing varying mol% of Cibalackrot with TADF material 4CzIPN or 4CzIPN-^tBu. a) ternary blends containing TADF:CBP \approx 30:70 mol%, or b) a binary blend with TADF material. All films were spin-coated from 0.5 wt% chloroform solution.

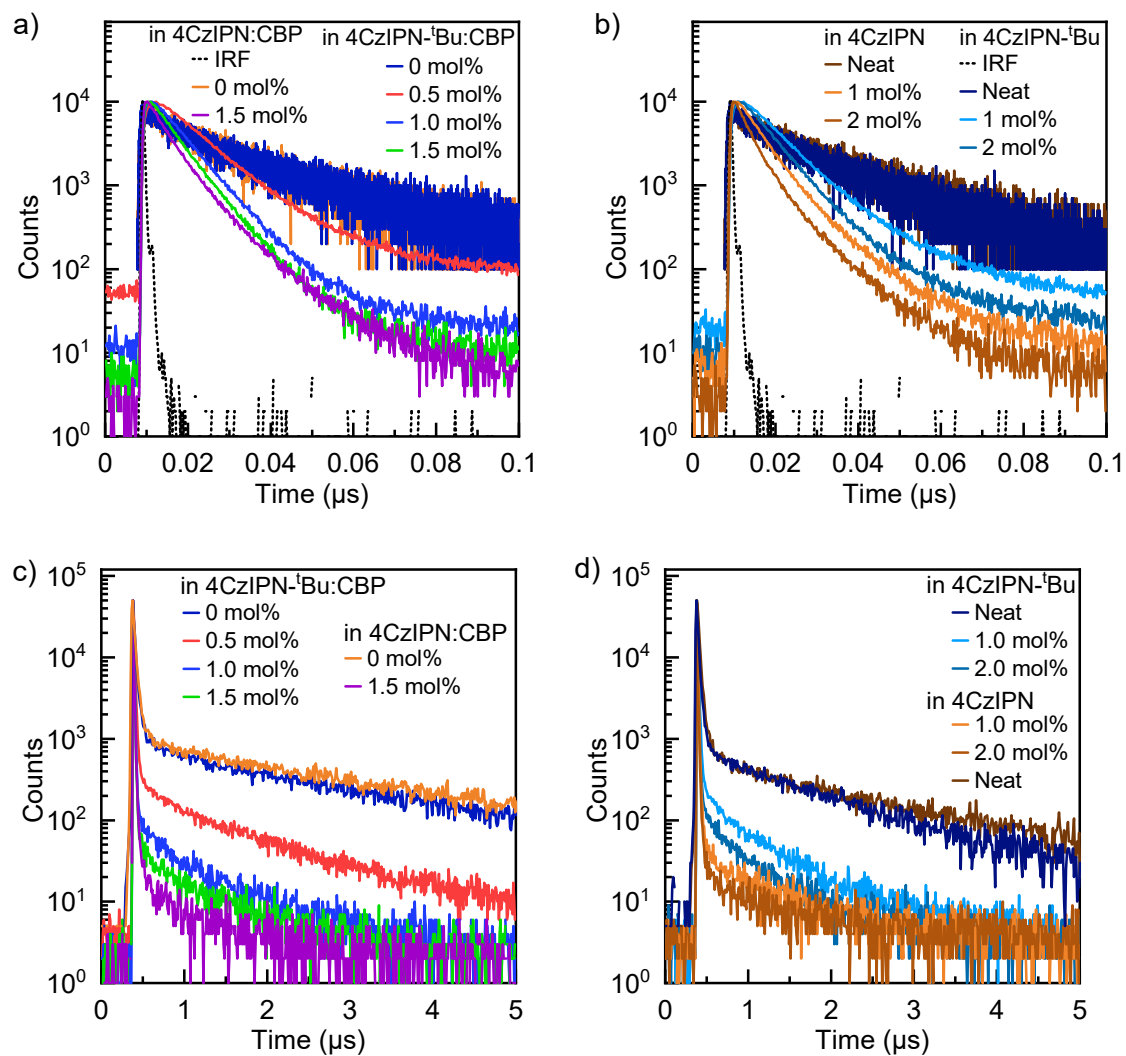


Figure S3 Solid state TCSPC prompt and delayed fluorescence decay of thin films containing varying mol% of Cibalackrot with a TADF material of 4CzIPN or 4CzIPN-^tBu. a) Prompt fluorescence decay of ternary blends containing TADF:CBP \approx 30:70 mol%, compared with binary blends of TADF:host, b) prompt fluorescence decay of binary blend with TADF material, c) delayed fluorescence decay of ternary blends, and d) delayed fluorescence decay of binary blends. All films were spin-coated from 0.5 wt% chloroform solution.

Blend Ratio (mol%)			Host	λ_{Abs} (nm)	λ_{PL} (nm)	PLQY (%)	τ_p (ns)	τ_d (ns)
Cibalackrot	TADF							
0.5	29.5	4CzIPN- ^t Bu	CBP	295, 330 (343 sh), 390 (462 sh)	540, 598 (639 sh)	79	18.5	836
1.0	29.0	4CzIPN- ^t Bu	CBP	295, 330 (343 sh), 390 (462 sh)	603 (642 sh)	77	9.7	564
1.5	28.5	4CzIPN- ^t Bu	CBP	295, 330 (343 sh), 390 (462 sh)	606 (647 sh)	74	7.2	603
1.5	28.5	4CzIPN	CBP	295, 327 (344 sh), 378 (454 sh)	609 (649 sh)	69	6.68	509
1.0	99.0	4CzIPN- ^t Bu	–	292, 320, 332, 386 (452 sh)	590 (631 sh)	70	12.8	562
2.0	98.0	4CzIPN- ^t Bu	–	292, 320, 332, 386 (452 sh)	592 (632 sh)	65	9.32	469
1.0	99.0	4CzIPN	–	289, 316, 327, 382, (450 sh)	604 (640 sh)	58	7.44	618
2.0	98.0	4CzIPN	–	289, 316, 327, 382, (450 sh)	606 (649 sh)	47	5.72	498

Table S3 Photophysical properties of Cibalackrot B blend films

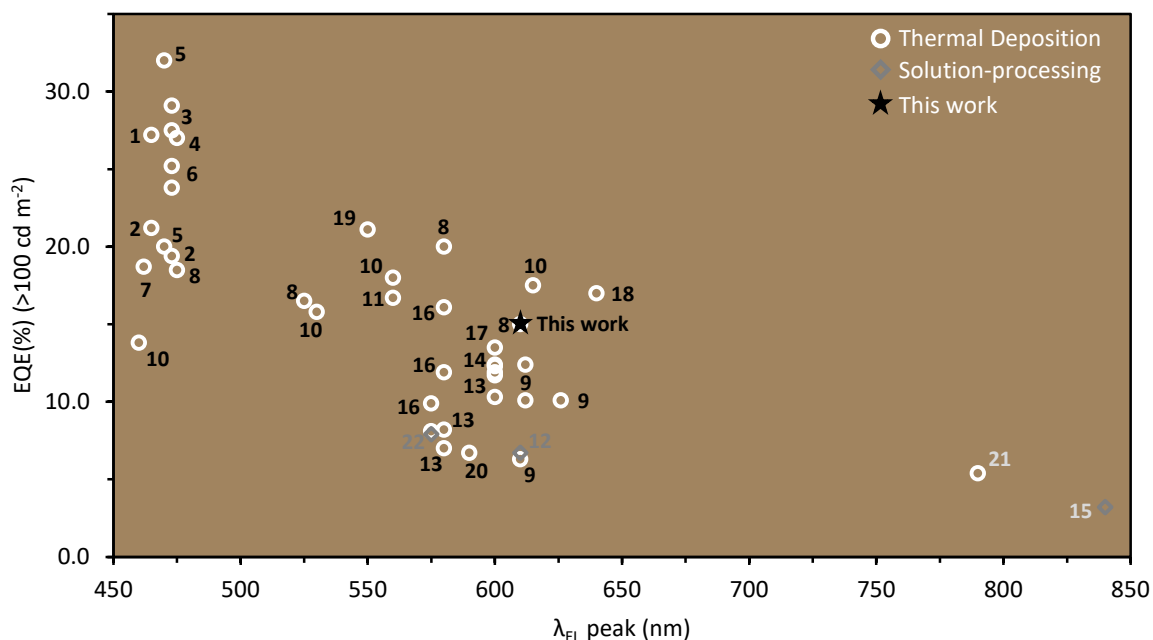


Figure S4 EQEs (%) ($>100 \text{ cd m}^{-2}$) of hyperfluorescent OLEDs *versus* electroluminescent peak wavelength (λ_{EL}) (nm). White circles represent devices fabricated by using thermal deposition, grey diamonds represent devices fabricated by using solution processing, and the black star represents this work. Reference according to number label.¹⁻²²

References

1. S. H. Han, J. H. Jeong, J. W. Yoo and J. Y. Lee, *J. Mater. Chem. C*, 2019, **7**, 3082-3089.
2. Y. T. Lee, C. Y. Chan, M. Tanaka, M. Mamada, U. Balijapalli, Y. Tsuchiya, H. Nakanotani, T. Hatakeyama and C. Adachi, *Adv. Electron. Mater.*, 2021, **7**, 2001090.
3. R. Braveenth, H. Lee, J. D. Park, K. J. Yang, S. J. Hwang, K. R. Naveen, R. Lampande and J. H. Kwon, *Adv. Funct. Mater.*, 2021, 202105805.
4. K. Stavrou, A. Danos, T. Hama, T. Hatakeyama and A. Monkman, *ACS Appl. Mater. Interfaces*, 2021, **13**, 8643–8655.
5. C.-Y. Chan, M. Tanaka, Y.-T. Lee, Y.-W. Wong, H. Nakanotani, T. Hatakeyama and C. Adachi, *Nat. Photonics*, 2021, **15**, 203–207.
6. S. O. Jeon, K. H. Lee, J. S. Kim, S.-G. Ihn, Y. S. Chung, J. W. Kim, H. Lee, S. Kim, H. Choi and J. Y. Lee, *Nat. Photonics*, 2021, **15**, 208–215.
7. Y. Wada, H. Nakagawa, S. Matsumoto, Y. Wakisaka and H. Kaji, *Nat. Photonics*, 2020, **14**, 643–649.
8. L.-S. Cui, A. J. Gillett, S.-F. Zhang, H. Ye, Y. Liu, X.-K. Chen, Z.-S. Lin, E. W. Evans, W. K. Myers, T. K. Ronson, H. Nakanotani, S. Reineke, J.-L. Bredas, C. Adachi and R. H. Friend, *Nat. Photonics*, 2020, **14**, 636–642.
9. Y.-K. Wang, C.-C. Huang, S. Kumar, S.-F. Wu, Y. Yuan, A. Khan, Z.-Q. Jiang, M.-K. Fung and L.-S. Liao, *Mater. Chem. Front.*, 2019, **3**, 161–167.
10. H. Nakanotani, T. Higuchi, T. Furukawa, K. Masui, K. Morimoto, M. Numata, H. Tanaka, Y. Sagara, T. Yasuda and C. Adachi, *Nat. Commun.*, 2014, **5**, 4016–4016.
11. T. Furukawa, H. Nakanotani, M. Inoue and C. Adachi, *Sci. Rep.*, 2015, **5**, 8429-8429.
12. D. Chen, X. Cai, X.-L. Li, Z. He, C. Cai, D. Chen and S.-J. Su, *J. Mater. Chem. C*, 2017, **5**, 5223–5231.
13. J. H. Kim, K. H. Lee and J. Y. Lee, *Chem. Eur. J.*, 2019, **25**, 9060–9070.
14. D. Li, Y. Hu and L.-S. Liao, *J. Mater. Chem. C.*, 2019, **7**, 977–985.
15. A. Shahalizad, A. Malinge, L. Hu, G. Laflamme, L. Haeblerlé, D. M. Myers, J. Mao, W. G. Skene and S. Kéna-Cohen, *Adv. Funct. Mater.*, 2021, **31**, 2007119.
16. H. H. Cho, A. S. Romanov, M. Bochmann, N. C. Greenham and D. Credgington, *Adv. Opt. Mater.*, 2021, **9**, 2001965.
17. H. S. Kim, S. H. Lee, J. Y. Lee, S. Yoo and M. C. Suh, *J. Phys. Chem. C*, 2019, **123**, 18283–18293.
18. M. Tanaka, R. Nagata, H. Nakanotani and C. Adachi, *ACS Appl. Mater. Interfaces*, 2020, **12**, 50668–50674.
19. B. Yurash, H. Nakanotani, Y. Olivier, D. Beljonne, C. Adachi and T. Q. Nguyen, *Adv. Mater.*, 2019, **31**, 1804490.
20. Y. J. Cho, K. S. Yook and J. Y. Lee, *Adv. Mater.*, 2014, **26**, 6642–6646.
21. J. Brodeur, L. Hu, A. Malinge, E. Eizner, W. G. Skene and S. Kéna-Cohen, *Adv. Opt. Mater.*, 2019, **7**, 1901144.
22. A. Shukla, S. K. M. McGregor, R. Wawrzinek, S. Saggari, E. G. Moore, S.-C. Lo and E. B. Namdas, *Adv. Funct. Mater.*, 2021, **31**, 2009817.